Biochemical Engineering Journal 17 (2004) 155–167

Biochemical Engineering Journal

www.elsevier.com/locate/bej

Advances in understanding and modeling the gas–liquid mass transfer in shake flasks

Ulrike Maier, Mario Losen, Jochen Büchs*

Biochemical Engineering, RWTH Aachen University, Worringerweg 1, Aachen 52056, Germany

Received 12 December 2001; accepted after revision 17 June 2003

Abstract

The gas–liquid mass transfer in 250 ml shake flasks has previously been sucessfully modelled on basis of Higbie's penetration theory. The current contribution presents advances in understanding and modelling the gas–liquid mass transfer in shake flasks at waterlike liquid viscosity in flask sizes between 50 and 1000 ml. An experimental investigation of the maximum gas–liquid mass transfer capacity OTR_{max} using the sodium sulphite system was extended to relative filling volumes of 4–16%, shaking diameters of 1.25, 2.5, 5, 7, 10 cm and shaking frequencies of 50–500 rpm for the above flask sizes. Simultaneously, the previous model of the gas–liquid mass transfer was extended to a "two sub-reactor model" to account for different mechanisms of mass transfer in the liquid film on the flask wall and the bulk of the liquid rotating within the flask. The shake flask is for the first time considered to be a two-reactor system consisting of a stirred tank reactor (bulk liquid) and a film reactor (film on flask wall and base). The mass transfer into the film on the flask wall and base at "in-phase" operating conditions is described by Higbie's penetration theory. Two different mass transfer theories were applied to successfully describe the mass transfer into the bulk liquid: a model by Kawase and Moo-Young and a model by Gnielinski. The agreement between the new modelling approach, which requires absolutely no fitting parameters and the experimental is within ±30%. The applicability of the models to a biological system was shown using a *Pichia pastoris* culture. This is particularly notable since geometrically non-similar liquid distributions in very different sizes of shaking flasks are covered. A comparable description of the gas–liquid mass transfer in bubble aerated reactors like stirred tanks is absolutely out of reach. A spatially- and time-resolved consideration of the mass transfer in the liquid film on the flask wall and base has shown that the validity of Higbie's theory sensitively depends on the film thickness and contact time.

Keywords: Gas–liquid mass transfer; Shake flasks; Modelling; Aeration; Aerobic processes; Bioprocess engineering

1. Introduction

Providing sufficient oxygen to biological cultures is vital for efficient bioprocess development. According to Hilton [1], "highly variable fermentation processes may constructively be viewed as the result of a lack of awareness of some parameter critical to that particular process. Often in small liquid batch processes, that critical parameter is gas exchange or balance between respiration rate (oxygen demand of the culture, OUR) and oxygen transfer (to the culture, OTR)". The oxygen demand of the culture OUR may be limited if it exceeds the maximum oxygen transfer capacity OTR_{max} through the shake flask closure and the gas–liquid interface. If the metabolism of the organism under investigation remains unaffected by the oxygen limitation, the observed growth rate is a function of the mass transfer rate alone and gives no information about the true growth rate of the microorganisms as demonstrated by van Suijdam et al. [2]. Yet, changes in metabolism may occur [3]. Büchs [4] has identified different degrees of severity of the metabolic problems encountered resulting from an oxygen limitation. In summary it can be said that the true effect of the variables under study in the screening stage of bioprocess development may be difficult to evaluate under oxygen limitation [5]. Only when the operating conditions are changed in such a way as to increase OTR_{max} does the true and unlimited oxygen uptake rate OUR, meaning the unlimited breathing rate, of the microorganisms become visible. Screening under an unknown oxygen limitation may cause an unwanted selection pressure and thus lead to a high degree of variability in an early and decisive stage of bioprocess development. To harmonise screening experiments, suitable operating conditions (flask size, shaking frequency, filling volume and shaking diameter) ensuring sufficient oxygen supply to cultures must be determined. For this it is vital to gain a

* Corresponding author. Present address: Biochemical Engineering, RWTH Aachen University, Worringerweg 1, Aachen 52056, Germany. Tel.: +49-241-8025546; fax: +49-241-8022265.
E-mail address: buechs@biovt.rwth-aachen.de (J. Büchs).

1369-703X/$ – see front matter © 2003 Elsevier B.V. All rights reserved.
doi:10.1016/S1369-703X(03)00174-8

Nomenclature

a	specific mass transfer area (m^2/m^3)
a_i	specific mass transfer area of differential slice (m^2/m^3)
a_i^B	specific mass transfer area of bulk (m^2/m^3)
a_i^F	specific mass transfer area of differential slice of film (m^2/m^3)
c_{cat}	catalyst concentration (mol/m^3)
$c_{O_2,b}$	dissolved oxygen concentration of liquid bulk (mol/m^3)
c_D	factor
$c^*_{O_2,L}$	oxygen concentration at gas–liquid interface (mol/m^3 or % air sat.)
$c_{O_2,L}$	dissolved oxygen concentration (mol/m^3 or % air sat.)
c_s	oxygen concentration in the liquid bulk (mol/m^3)
d	maximum shake flask diameter (m)
d_i	maximum shake flask diameter at considered height (m)
d_0	shaking diameter (m)
D_{O_2}	diffusion coefficient of oxygen in liquid phase (m^2/s)
dt	time step (1×10^{-4}) s
Fr_a	axial Froude number (−), [23]
k_L	gas–liquid mass transfer coefficient (m/s)
$k_{L,i}$	gas–liquid mass transfer coefficient for differential slice (m/s)
$k^B_{L,i}$	gas–liquid mass transfer coefficient of bulk (m/s)
$k^F_{L,i}$	gas–liquid mass transfer coefficient of film (m/s)
k_La	integral volumetric gas–liquid mass transfer coefficient (1/s)
k_n	reaction rate constant nth order ($1/s(m^3/mol)^{n-1}$)
L	characteristic overflow length (m)
L_i	characteristic overflow length of each differential slice (m)
L_{O_2}	oxygen solubility (mol/(l bar))
n	shaking frequency (1/s or rpm) reaction order of sulphite reaction with respect to oxygen
$\bar{\dot{n}}_{O_2}$	time averaged oxygen flux across the gas–liquid interface (mol/s)
$\bar{\dot{n}}_{O_2,Higbie}$	time averaged oxygen flux across the gas–liquid interface according to Higbie's penetration theory (mol/s)
OTR	oxygen transfer rate ($mol/(m^3\,s)$)
OTR_B	oxygen transfer rate of biological system ($mol/(m^3\,s)$)
OTR_{max}	maximum oxygen transfer capacity ($mol/(m^3\,s)$)
$OTR_{max,i}$	maximum oxygen transfer capacity of differential slice ($mol/(m^3\,s)$)
$OTR^B_{max,i}$	maximum oxygen transfer capacity of bulk slice ($mol/(m^3\,s)$)
$OTR^F_{max,i}$	maximum oxygen transfer capacity of film slice ($mol/(m^3\,s)$)
Ph	Phase number, [23]
$p_{O_2,G}$	oxygen partial pressure in gas-phase (bar)
$p_{O_2,L}$	oxygen partial pressure in liquid-phase (bar)
Re	Reynolds number, $Re = (d^2n)/\upsilon(-)$
Re_L	overflow Reynolds number, Eq. (10) (−)
Sc	Schmidt number, $Sc = \eta/(\rho D_{O_2})$ (−)
Sh_{min}	minimum Sherwood number
Sh_{lam}	laminar Sherwood number, Eq. (8)
Sh_{turb}	turbulent Sherwood number, Eq. (9)
t_c	contact time (s)
$t^B_{c,i}$	contact time of bulk liquid (s)
$t^F_{c,i}$	contact time of liquid film (s)
υ	velocity of the liquid surface relative to the flask wall
V_L	filling volume (m3)
x	length scale perpendicular to wall (m)

Greek symbols

δ	film thickness (m)
$\tilde{\varepsilon}$	energy dissipation rate (W/kg)
ε_{rel}	relative deviation between oxygen flux calculated using Higbie's penetration theory and of exact solution of mass transfer equation (%)
η	viscosity of liquid phase (mPa s)
ν	kinematic viscosity of liquid phase (kg m/s)
ρ	density of liquid (kg/m^3)

mechanistic understanding of the gas–liquid mass transfer, meaning the maximum oxygen transfer capacity OTR_{max} of the shake flask in dependency of the influencing factors.

Oxygen transfer in shake flasks has previously been discussed in the literature [2,8–12]. Frequently a chemical model system, such as the sodium sulphite system has been employed to simulate a biological oxygen consumer in experimental investigations. Yet, the results of the investigations conducted are difficult to transfer to every day laboratory work in a biological system since only a limited range of operating conditions (flask size, filling volume, shaking diameter, shaking frequency) has been investigated [7]. In some investigations oxygen probes immersed in the liquid have influenced the hydrodynamics and thus the gas–liquid mass transfer characteristics of the system [5,8] making results difficult to interpret. Vital

information such as the diffusion coefficient D_{O_2} and oxygen solubility L_{O_2} of the chemical model system investigated often lacks, so that data cannot be employed to identify suitable operating conditions for a specific biological system.

In a previous approach [7] a fully mechanistic understanding of the gas–liquid mass transfer in 250 ml shake flasks requiring absolutely no fitting parameters was developed. The aim of this current investigation is to extend the previous understanding of the gas–liquid mass transfer to a wider range of operating conditions at waterlike liquid viscosity. For this the OTR_{max} was investigated experimentally using a fully defined chemical system (aqueous sodium sulphite) which simulates a biological oxygen consumer.

2. Theory

2.1. Gas–liquid mass transfer into shake flasks

The mass transfer into the shake flask is described by two resistances: that of the closure and that of the gas–liquid interface. The influence of the sterile closure on the oxygen partial pressure in the flask has been studied in detail by Mrotzek et al. [6]. The results presented in the following will only be concerned with the maximum transfer properties across the gas–liquid interface. An overview over literature and first results concerning the gas–liquid mass transfer have been previously presented [7]. The basic mass transfer correlations will be briefly presented in the following.

The oxygen transfer rate OTR is proportional to the mass transfer coefficient k_L, the specific transfer area a, the oxygen solubility L_{O_2} and the driving pressure difference $p_{O_2,G} - p_{O_2,L}$ or driving concentration difference $c^*_{O_2,L} - c_{O_2,L}$ across the gas–liquid interface

$$OTR = k_L a\, L_{O_2}(p_{O_2,G} - p_{O_2,L}) = k_L a(c^*_{O_2,L} - c_{O_2,L}) \quad (1)$$

The OTR defined by Eq. (1) is at its maximum, when the driving partial pressure or concentration difference is greatest. This is the case when the closure resistance can be neglected and the oxygen partial pressure $p_{O_2,L}$ or the dissolved oxygen concentration $c_{O_2,L}$ in Eq. (1) is equal to 0. The oxygen transfer rate OTR at this point is termed as the maximum oxygen transfer capacity OTR_{max}

$$OTR_{max} = k_L a\, L_{O_2}\, p_{O_2,G} = k_L a\, c^*_{O_2,L} \quad (2)$$

The factors influencing k_L, L_{O_2} and a have been discussed previously [7].

2.2. Previous mechanistic model of the gas–liquid mass transfer

The previous mechanistic understanding of the gas–liquid mass transfer in shake flasks is based on a model of the liquid distribution [7,17]. In this model the movement of the shaking table is divided into two partial movements as shown in Fig. 1a, the movement of the flask around the excenter axis ω_1, and the opposite movement at the same angular velocity around the flask axis ω_2. The alignment of the flask remains unchanged in the North–South direction.

The liquid distribution results as the intersection between the rotational paraboloid based on a frictionless fluid and the flask wall. This model describes the liquid distribution and resulting gas–liquid mass transfer area a in the shake flask for liquids of low liquid viscosity [7]. In our previous investigation it was shown that the relevant mass transfer a in the shake flask comprises the mass transfer area of the bulk liquid a^B and the liquid film a^F distributed on the flask wall and base by the rotating bulk [7]. Using the above model of the liquid distribution to calculate the mass transfer area a, the maximum oxygen transfer capacity OTR_{max} can be calculated using Eq. (1) if the mass transfer coefficient k_L is known. Higbie's penetration theory [18] has previously [7] been applied to calculate the mass transfer coefficient k_L. In the shake flask the contact time $t_{c,i}$ between the gas and liquid phase depends on the considered height, meaning it is necessary to calculate the mass transfer coefficient in differential slices $k_{L,i}$, as shown in Fig. 1b. According to Higbie, the mass transfer coefficient is inversely proportional to the square root of the contact time $t_{c,i}$ between the gas- and liquid-phase

$$k_{L,i} = 2\sqrt{\frac{D_{O_2}}{\pi t_{c,i}}} \quad (3)$$

Higbie is valid for semi-infinite space, meaning that mass transfer takes place only close to the gas–liquid surface. The diffusion coefficient D_{O_2} for electrolyte solutions can be calculated according to Akita et al. [19] (see Table 1 for details).

In the mass transfer model [7] it was furthermore differentiated between

- the mass transfer coefficient $k^F_{L,i}$ of the liquid film, which is described by the contact time between the liquid film on the flask wall/base and gas phase $t^F_{c,i}$ (see Fig. 1b) and

Table 1
Input values for "gPROMS" simulation

	Nomenclature	Value
c^*_{L,O_2}	Oxygen concentration at gas–liquid interface	1.09×10^{-1} mol/m^3 [20]
c_s	Oxygen concentration in the liquid bulk	0 mol/m^3
dt	Time step	1×10^{-4} s[a]
D_{O_2}	Diffusion coefficient of oxygen in liquid phase (m^2/s)	1.22×10^{-4} m^2/s [19]
k_1	First-order reaction rate constant	0.52 1/s
δ	Film thickness	5×10^{-5} m

[a] d$t(n = 400) = 5 \times 10^{-5}$ s.

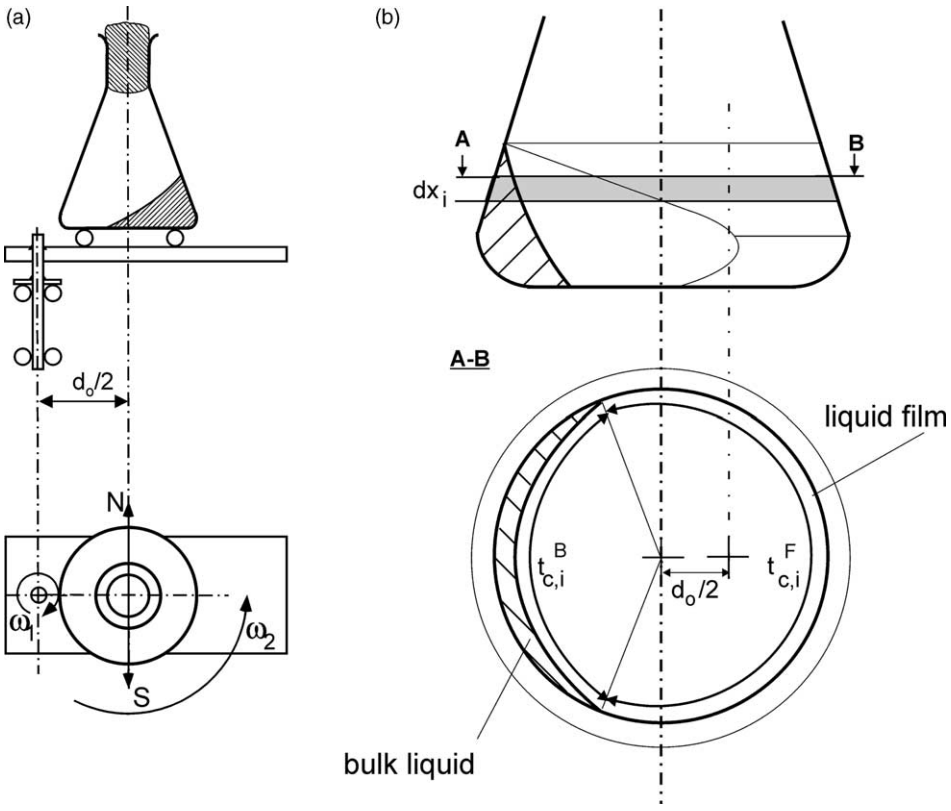

Fig. 1. Model of the liquid distribution and mass transfer in the shake flask: (a) division of the shaking movement into two partial movements—ω_1: rotation of the shaking table and ω_2: counter orientation of the shake flask; the combination of both movements results in a unchanged orientation of the shake flask relative to the ground; (b) application of Higbie's penetration theory to differential slice in the shake flask, d_0: shaking diameter, $t^{\mathrm{F}}_{\mathrm{c},i}$: film contact time, $t^{\mathrm{B}}_{\mathrm{c},i}$: bulk contact time.

- the mass transfer coefficient $k^{\mathrm{B}}_{\mathrm{L},i}$ of the bulk liquid, which is described by the contact time between the bulk surface and gas phase $t^{\mathrm{B}}_{\mathrm{c},i}$ (see Fig. 1b).

The contact time between the bulk surface and gas phase $t^{\mathrm{B}}_{\mathrm{c},i}$ is defined by the velocity of the liquid surface which is considered to move with the velocity of the flask wall v

$$t^{\mathrm{B}}_{\mathrm{c},i} = \frac{L_i}{v} \tag{4}$$

The maximum oxygen transfer capacity $\mathrm{OTR}_{\max}$ can now be calculated by inserting Eq. (3) into Eq. (1) with the respective mass transfer areas of the bulk liquid a^{B}_i and the film a^{F}_i resulting from the liquid distribution

$$\begin{aligned}\mathrm{OTR}_{\max} &= \underbrace{\sum_{i=1}^{N}\mathrm{OTR}^{\mathrm{F}}_{\max,i}}_{\text{film}} + \underbrace{\sum_{i=1}^{N}\mathrm{OTR}^{\mathrm{B}}_{\max,i}}_{\text{bulk}} \\ &= \left[\underbrace{\sum_{i=1}^{N}k^{\mathrm{F}}_{\mathrm{L},i}a^{\mathrm{F}}_i}_{\text{film}} + \underbrace{\sum_{i=1}^{N}k^{\mathrm{B}}_{\mathrm{L},i}a^{\mathrm{B}}_i}_{\text{bulk}}\right] c^{*}_{\mathrm{O_2,L}} = k_{\mathrm{L}}a\, c^{*}_{\mathrm{O_2,L}}\end{aligned} \tag{5}$$

The resulting mass transfer coefficient $k_{\mathrm{L}}a$ in Eq. (5) can be interpreted as an integral mass transfer coefficient comprising of the bulk and film contribution to the mass transfer. The dissolved oxygen concentration at the gas–liquid interface $c^{*}_{\mathrm{O_2,L}}$ can be calculated according to Schumpe et al. [20]. This mechanistic model of the mass transfer has been verified with some experimental data of limited range in the 250 ml shake flask [7].

2.3. Extended modelling approach

2.3.1. Model for mass transfer coefficient k_L according to Kawase and Moo-Young

The model described by Kawase and Moo-Young [26] is based on the periodic sublayer theory by Pinczewski and Sideman [27]. In this model, the mass transfer coefficient in surface aerated stirred tank bioreactors at conditions of isotropic turbulence is described by the following correlation:

$$k^{\mathrm{B}}_{\mathrm{L}} = 0.138 Sc^{-2/3}\left[\nu\tilde{\varepsilon}\right]^{1/4} = 0.138 Sc^{-2/3}\left[\nu\left(\frac{P}{V_{\mathrm{L}}\rho}\right)\right]^{1/4} \tag{6}$$

with the Schmidt number Sc, the kinematic viscosity of liquid phase ν, the energy dissipation rate $\tilde{\varepsilon}$ and the specific power input P/V_{L}.

2.3.2. Mass transfer model according to Gnielinski

A second model applied to calculate the mass transfer coefficient of the bulk liquid k_L^B is proposed. It is based on Gnielinski's [29] boundary layer theory in form of the Sherwood number $Sh = f(Re, Sc)$ valid for the liquid–solid mass transfer at a plane surface

$$\frac{k_L^B L}{D_{O_2}} = Sh_{min} + \sqrt{Sh_{lam}^2 + Sh_{turb}^2} \quad (7)$$

with the minimum Sherwood number $Sh_{min} = 8/\pi$ for a disc at diffusive conditions [29] and the laminar term Sh_{lam}

$$Sh_{lam} = 0.664 Re_L^{1/2} Sc_L^{1/3} \quad (8)$$

and the turbulent term Sh_{turb}

$$Sh_{turb} = \frac{0.037 Re_L^{0.8} Sc}{1 + 2.443 Re_L^{-0.1}(Sc^{2/3} - 1)} \quad (9)$$

with the characteristic overflow length L, the minimum Sherwood number Sh_{min} and the Schmidt number Sc. The overflow Reynolds number Re_L is defined by

$$Re_L = \frac{\rho L v}{\eta} \quad (10)$$

The above model can be transferred to any geometry by defining a characteristic overflow length L and velocity v [29]. In literature some investigators have carried fixed interface theories over to free surfaces [30], as for example Kawase and Moo-Young [26]. The "periodic transitional sublayer" theory [27] developed for liquid–solid mass transfer is directly transferred to the gas–liquid mass transfer at the free surface of a surface aerated bioreactor without the use of any fitting parameters. The gas–liquid interface is assumed to behave as a rigid boundary [26]. Kudrjawizki and Bauer [31], who investigated the gas–liquid mass transfer across a surface aerated stirred tank reactor also assume that the free surface behaves as a rigid boundary. On basis of this literature, Gnielinski's model, developed for solid–liquid mass transfer, is transferred to the gas–liquid interface of the bulk liquid by assuming that the gas–liquid interface behaves as a rigid boundary.

2.4. Gas–liquid mass transfer in liquid film

On basis of a first order reaction the oxygen mass balance around an element in a liquid film is described by

$$\frac{\partial c_{O_2,L}}{\partial t} = D_{O_2} \frac{\partial^2 c_{O_2,L}}{\partial x^2} - k_1 c_{O_2,L} \quad (11)$$

with the boundary conditions (see Fig. 2)

$$\text{BC1}: \quad c_{O_2,L}(x = 0) = c^*_{O_2,L}$$

$$\text{BC2}: \quad \left[\frac{\partial c_{O_2,L}}{\partial x}\right]_{x=\partial} = 0$$

$$\text{BC3}: \quad c_{O_2,L}(t_c = 0, x) = c_{O_2,b}$$

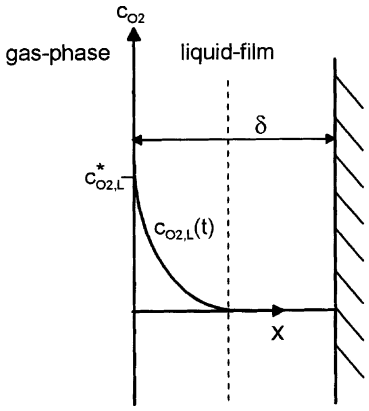

Fig. 2. Dissolved oxygen concentration profile in liquid film—$c^*_{O_2,L}$: oxygen concetration at gas–liquid interface; $c^*_{O_2,L}$: dissolved oxygen concentration at $t_c = 0$; δ: film thickness; x: length scale perpendicular to wall.

The inhomogeneous differential equation Eq. (11) can be solved using a simulation tool, such as "gPROMS" (Process Systems Enterprise Ltd., London, UK). Concentration profiles $c_{O_2,L}(x, t_c)$ which depend on contact time t_c and penetration depth result. The oxygen flux across the gas–liquid interface $\dot{n}_{O_2}$ can be calculated by

$$\dot{n}_{O_2}(x = 0, t) = \left[\frac{\partial c_{O_2,L}}{\partial x}\right]_{x=0,t} a D_{O_2} \quad (12)$$

with the exchange area a and the diffusion coefficient of oxygen D_{O_2}. The average oxygen flux across the gas–liquid interface $\bar{\dot{n}}_{O_2}$ within the contact time t_c is then given by

$$\bar{\dot{n}}_{O_2} = \frac{\int \dot{n}_{O_2}(x = 0, t)\, dt}{t_c} \quad (13)$$

According to Higbie the average oxygen flux across the gas liquid interface $\bar{\dot{n}}_{O_2,Higbie}$ is equal to

$$\bar{\dot{n}}_{O_2,Higbie} = 2\sqrt{\frac{D_{O_2}}{\pi t_c}} a c^*_{O_2,L} \quad (14)$$

2.5. The sodium sulphite system

The sodium sulphite reacts with the oxygen passing into the liquid according to the following reaction:

$$SO_3^{2-} + 0.5 O_2 \xrightarrow{Co^{2+}} SO_4^{2-} \quad (15)$$

To determine the mass transfer coefficient $k_L a$ from measurements of the absorption rate measurements have to be conducted in the so-called "non-accelerated" reaction regime described in detail by Linek and Vacek [16].

3. Materials and methods

3.1. The chemical model system

The chemical system used to simulate an oxygen consumer is a 1 M sodium sulphite system (≥98%, Roth,

Karlsruhe, Germany) in deionized water catalysed by 1×10^{-7} M cobalt sulphate (≥97.5%, Fluka Chemie AG, Buchs, Switzerland). The catalyst concentration of 1×10^{-7} M required to work in the "non-accelerated" reaction regime [16] was verified in preliminary experiments. The system is buffered using a 0.1 M phosphate buffer (disodiumhydrogenphosphate ≥99%; sodiumdihydrogenphosphate monohydrate ≥98%: Roth, Karlsruhe, Germany) to ensure a constant pH [13]. The system is adjusted to pH = 8 using sulphuric acid (≥30%, Applichem, Darmstadt, Germany) and has a resulting viscosity of $\eta = 1.78$ mPa s and a density of $\rho = 1105.9$ kg/m^3.

3.2. Investigation of the chemical model system

An investigation to determine the reaction kinetics of the sodium sulphite system was conducted in a 1.5 l stirred tank reactor (VSF Fermentor, Bioengineering, Wald, Switzerland) equipped with a polarographic gas analyzer (Model 26082, Orbisphere Laboratorien, Genf, Switzerland). The dissolved oxygen concentration $c_{O_2,L}$ was measured with an oxygen sensor (Comp. Nr. 341003050, Mettler Toledo, Steinbach, Germany). The reactor was aerated at 1.15 vvm and operated at a temperature of $T = 22.5\,^{\circ}$C. The stirring speed was increased in steps from 400 to 800, 1200, 1500 and 2000 rpm keeping each stirring speed constant until the oxygen transfer rate OTR and the dissolved oxygen concentration $c_{O_2,L}$ were in steady state. For each stirring speed, corresponding values of OTR and $c_{O_2,L}$ were gained. The experiment was conducted at a cobalt catalyst concentration c_{cat} equal to 0, 1×10^{-7}, 1×10^{-6} and 1×10^{-5} M.

3.3. Biological experiments

Pichia pastoris was grown on complex medium (YPG: 10 g/l glycerine, Applichem, Darmstadt, Germany, 10 g/l select yeast extract, Chemie AG, Buchs, Switzerland and 20 g/l select peptone, Gibco BRL, Invitrogen Life Technologies, Karlsruhe, Germany; YPM: 31.64 g/l methanol, Aldrich, Steinheim, Germany, 10 g/l select yeast extract, Gibco BRL, Invitrogen Life Technologies, Karlsruhe, Germany and 20 g/l peptone, Invitrogen Life Technologies, Karlsruhe, Germany). The culture was run into an oxygen limitation verified by carrying out the experiment using the online measuring method described by Anderlei and co-workers [3,21,22]. The experiment was conducted in a 250 ml shake flask at 5 cm shaking diameter, 10, 15, 25 and 40 ml filling volume and 50–500 rpm shaking frequency (in steps of 50) at a temperature of $T = 30\,^{\circ}$C.

3.4. Shake flask experiments

The OTR was measured using an on-line measuring method developed by Anderlei and co-workers [3,21,22,32]. Erlenmeyer flasks of 50, 100, 250, 500, and 1000 ml nominal volume, relative filling volumes of 4–16%, shaking diameters of 1.25, 2.5, 5, 7, 10 cm (modified Lab Shaker, Kühner AG, Birsfelden, Switzerland) and shaking frequencies of 50–500 rpm (in 50 rpm steps) at waterlike liquid viscosity were investigated. The investigations were carried out at a temperature of $T = 22.5\,^{\circ}$C. For calculation of k_La the oxygen solubility and diffusion coefficient given in Table 1 was used.

4. Results and discussion

4.1. Investigation of the chemical model system

An investigation was conducted in a stirred tank reactor to determine the reaction kinetics of the sodium sulphite system according to Eq. (16). The measuring points of the OTR in Fig. 3 were fitted to the following equation in a least-squares sense:

$$\mathrm{OTR} = k_n c_{O_2,L}^{n} \tag{16}$$

The measured oxygen transfer rate OTR describes the oxygen balance around the liquid, k_n in Eq. (16) can be considered as the reaction rate constant and n as the reaction order of the sulphite reaction.

From Fig. 3 it can be seen that the reaction order of the sulphite reaction increases from 1 (when no catalyst is present) in direction of 2 with increasing catalyst concentration. This effect has also been reported in literature [14–16]. For the catalyst concentration of 10^{-7} M applied in the systematic investigation of the shake flask in this work, the reaction order is $n = 1.1$ and the reaction rate constant is $k_n = 0.7$ 1/s (m^3/mol)$^{n-1}$. Fig. 3 furthermore shows that the dissolved oxygen concentration $c_{O_2,L}$ is actually unequal to 0 for all catalyst concentrations investigated. This means that the measured OTR (Eq. (1)) does not correspond with the maximum oxygen transfer capacity OTR_{max} (Eq. (2)), which assumes a dissolved oxygen concentration $c_{O_2,L}$ of 0. This is quite in contrast to literature, which assumes that the sodium sulphite system reduces the dissolved oxygen concentration to 0 in the so called "non-accelerated" reaction regime [16], in which investigations of the volumetric gas–liquid mass transfer coefficient k_La should be conducted. Consequently, the measured oxygen transfer rate OTR in this investigation is based on a significantly lower driving concentration difference than if the full driving concentration difference (at $c_{O_2,L} = 0$) were achieved. Still, the measured oxygen transfer rate OTR in the shake flask can be corrected to the maximum oxygen transfer capacity OTR_{max} by resolving Eq. (1) to the volumetric mass transfer coefficient k_La as follows:

$$k_La = \frac{\mathrm{OTR}}{c^*_{O_2,L} - c_{O_2,L}} \tag{17}$$

and inserting this expression into Eq. (2)

$$\mathrm{OTR}_{max} = \frac{\mathrm{OTR}}{c^*_{O_2,L} - c_{O_2,L}} c^*_{O_2,L} \tag{18}$$

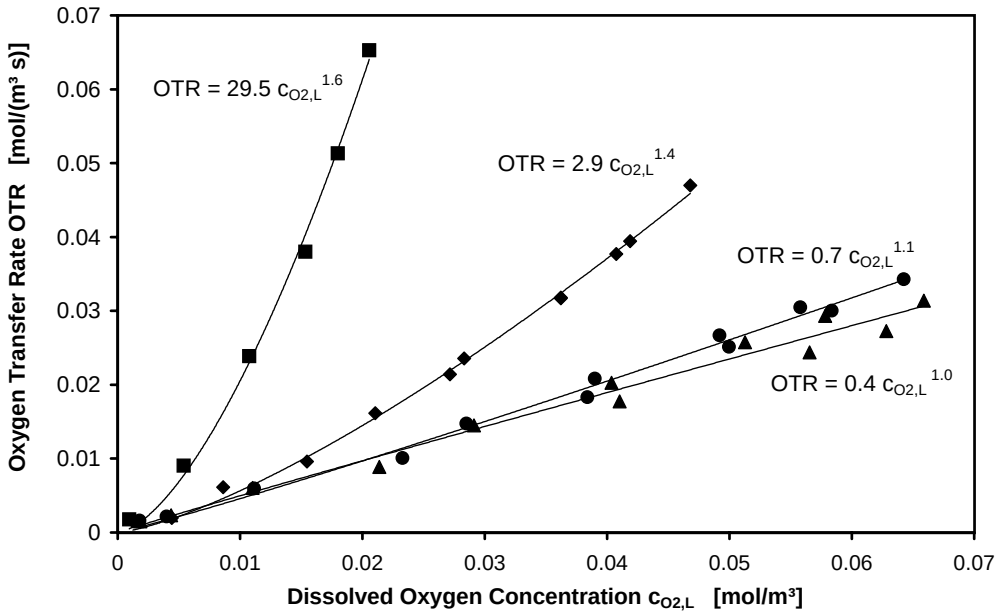

Fig. 3. Reaction kinetics of the 1 M sodium sulphite system: oxygen transfer rate, OTR vs. dissolved oxygen concentration $c_{O_2,L}$ under variation of the stirrer speed and cobalt sulfate catalyst concentration, 1.4 l stirred tank reactor, $T = 22.5\,^{\circ}C$, catalyst concentration: (■) $c = 10^{-5}$ M; (◆) $c = 10^{-6}$ M; (●) $c = 10^{-7}$ M; (▲) no catalyst.

In the shake flask the dissolved oxygen concentration $c_{O_2,L}$ in Eqs. (17) and (18) (depending on whether $k_L a$ or OTR_{max} is regarded) can be calculated from the oxygen mass balance in Eq. (16)

$$c_{O_2,L} = \sqrt[n]{\frac{OTR}{k_n}} \tag{19}$$

The oxygen concentration at the gas–liquid interface phase $c^*_{O_2,L}$ in Eqs. (17) and (18) can be calculated according to Schumpe et al. [20] (see Table 1 for details).

4.2. Transfer of data from chemical model system to biological system

The applicability of the measured results of the chemical model system to a biological system was verified using a *P. pastoris* culture. The comparison between the measured oxygen transfer rate OTR_B of the *P. pastoris* culture and the maximum oxygen transfer capacity OTR_{max} of the sodium sulphite system is shown in Fig. 4. OTR_B is in fact higher than OTR_{max} of the sodium sulphite system due to the lower ionic strength of the biological system. There is a linear

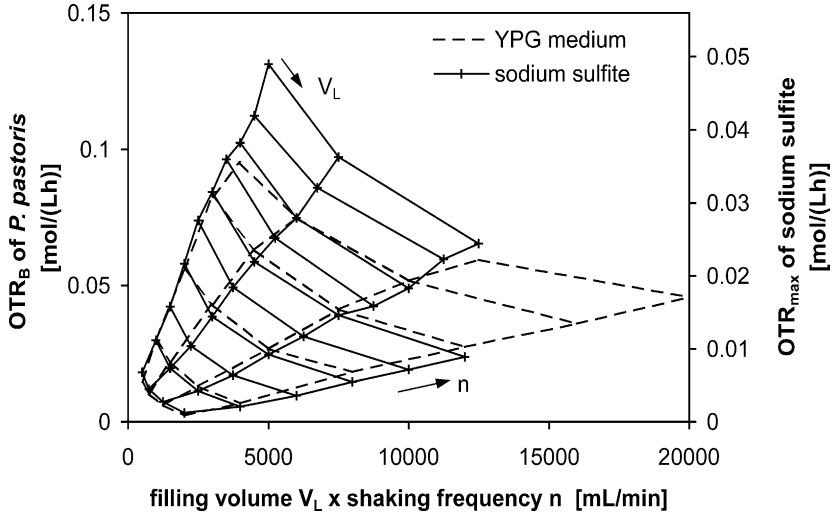

Fig. 4. Measured oxygen transfer rate OTR of *P. pastoris* vs. maximum oxygen transfer capacity OTR_{max} of sodium sulphite system calculated from Eq. (18): 250 ml shake flask, 5 cm shaking diameter, V_L = 10, 15, 25 and 40 ml, n = 50–500 rpm (in steps of 50), resulting correlation factor $OTR_B/OTR_{max} = 2.8$, $R^2 = 0.97$.

relationship between OTR_B of the *P. pastoris* culture and OTR_{max} of the sodium sulphite system. A correlation factor of $OTR_B/OTR_{max} = 2.8$ results over the investigated range of operating conditions. This shows that the 1 M sodium sulphite system is suitable to model *P. pastoris* as an oxygen consumer by applying one correlation factor for all operating conditions. The applicability to other biological systems requires different correlation factors which need to be individually determined for each system.

4.3. Systematic description of the gas–liquid mass transfer in shake flasks

The experimental investigation of OTR_{max} in the shake flask using the above described sodium sulphite system is extended well beyond the commonly applied operating conditions. The maximum volumetric mass transfer coefficient of the experimental investigation was found to be $k_La_{,Exp} = 0.157$ 1/s in the 50 ml flask at a relative filling volume of 4%, a shaking frequency of 450 rpm and shaking diameter of 7 cm.

The validity of the previous mechanistic model of the gas–liquid mass transfer described above and termed as "previous model" will now be investigated using the mass transfer coefficient k_La (model: Eq. (5) resolved to k_La; measuring values: Eq. (17)). The comparison between the volumetric mass transfer coefficient of the model computations k_La_{Model} and measurements k_La_{Exp} for the investigated operating conditions shows that although there is a general linear tendency the data points clearly scatter (data not shown). The average deviation of the model values from the measuring values is given by the linearly assumed fit $k_La_{Model} = 1.62k_La_{Exp}$ meaning 62% deviation. This means that Higbie's model applied for the bulk liquid and film mass transfer as in Eq. (3) overestimates the experimental data.

4.4. Extended modelling approach

When applying Higbie's theory to model the mass transfer coefficient of the bulk liquid $k^B_{L,i}$ ("previous model"), the surface of the bulk liquid is considered to move with the velocity of the flask wall, neglecting all friction effects within the liquid. Due to this, the bulk mass transfer is likely to be overestimated. According to power input investigations by Büchs and Zoels [25], the bulk can be considered as being well-mixed. This mixing in the liquid is not accounted for by Higbie's model. It is thus necessary to extend the modelling approach to account for the different mechanisms of mass transfer in the liquid film and bulk liquid. For this, the shake flask is divided into two hypothetical reactors: a falling film reactor and a stirred tank reactor as shown in Fig. 5.

It can be assumed at this point that Higbie's penetration theory, which has been specifically developed for falling films satisfactorily describes the film mass transfer coefficient k^F_L in Eq. (5). A suitable model to describe the mass transfer coefficient of the bulk liquid k^B_L in Eq. (5) must still

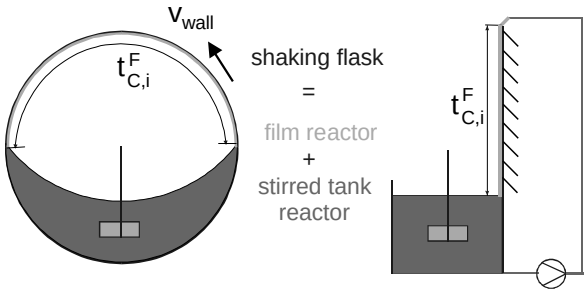

Fig. 5. Hydrodynamics in the liquid bulk and resulting "two sub-reactor model" of the shake flask: hypothetical division of the shake flask into a falling film and a stirred tank reactor.

be found. Several mass transfer models including models based on the "boundary layer theory", such as those by King [30], Lamont and Scott [32], Theofanous et al. [33], Prasher [34] and Zhang and Thomas [35] were therefore tested for their suitability to describe the mass transfer in the shake flask. These models proved to significantly overestimate the mass transfer coefficient of the liquid bulk. Only the models by Kawase and Moo-Young [26] and Gnielinski [29] lead to reasonable mass transfer coefficients as will be presented in the following.

4.4.1. Mass transfer model according to Kawase and Moo-Young

The first model proposed to describe the mass transfer into the bulk liquid is a model by Kawase and Moo-Young [26] according to Eq. (6). This correlation is transferred to the shake flask using the volumetric power input correlation described by Büchs et al. [23].

$$\frac{P}{V_L\rho} = \frac{n^3d^4}{V_L^{2/3}(70Re^{-1} + 25Re^{-0.6} + 1.5Re^{-0.2})} \tag{20}$$

with the shaking frequency n, the maximum flask diameter d and the Reynolds number Re. The conditions of isotropic turbulence were ensured using Liepe's criteria [28], which has been transferred to the shake flask by Büchs and Zoels [25].

Eq. (6) is now applied to calculate the mass transfer coefficient of the bulk liquid k^B_L. The bulk contribution to the total mass transfer in Eq. (5) is calculated using the specific exchange area of the bulk a^B. The film contribution in Eq. (5) is calculated with Higbie's penetration theory. This approach will be referred to as the "Kawase and Moo-Young two sub-reactor model". Fig. 6 shows the experimental versus the modelled values of the volumetric mass transfer coefficient.

If all measuring points are considered the scattering is still significant. To elucidate this behaviour the hydrodynamics of the measuring points are considered. In shake flasks the bulk of the liquid generally rotates with the direction of the centrifugal acceleration. Yet, an unfavourable hydrodynamic operating condition, the so-called "out-of-phase" condition

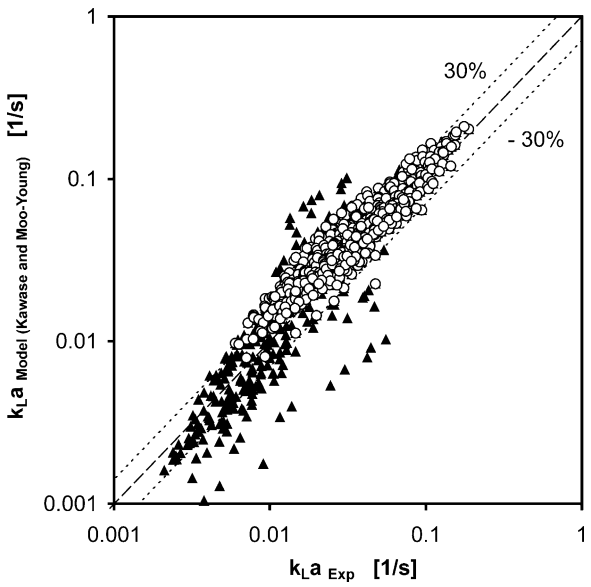

Fig. 6. Volumetric mass transfer coefficient of model $k_L a_{Model}$ (film mass transfer: Higbie; bulk mass transfer: Kawase and Moo-Young) vs. measuring values $k_L a_{Exp}$: 50–1000 ml shake flask, 1.25–10 cm shaking diameter, 4–20% relative filling volume, 50–500 rpm shaking frequency, 1 M sodium sulphite system, $T = 22.5\,^{\circ}C$, (▲) all measurement values; (○) only "in-phase" measurement values which were calculated according to Büchs et al. [23] with the Phase number, $Ph > 1.26$ and axial Froude number, $Fr_a > 0.4$, $k_L a_{Model} = 1.16 k_L a_{Exp}$; $R^2 = 0.88$.

[23] may occur towards small shaking diameters, low filling volumes and high liquid viscosities. At this operating condition, the bulk liquid no longer rotates with the direction of the centrifugal acceleration [23,24], but collapses at the flask base. The specific power input P/V_L and mass transfer area a are consequently significantly reduced. The model of the liquid distribution explained above, is unable describe the mass transfer area at "out-of-phase" operating conditions, since it assumes a symmetrical liquid bulk rotating within the flask. The "out-of-phase" operating conditions in our investigation can be identified and eliminated using the "in-phase" criteria by Büchs et al. [23]. With this the scattered data points are clearly reduced as Fig. 6 shows. It can be concluded that the scattering is obviously caused by the "out-of-phase" operating conditions. The average deviation of the model from the measured values is reduced from 60% in the "previous model" to 16%, meaning a correlation factor of 1.16.

4.4.2. Mass transfer model according to Gnielinski

To apply this model the bulk liquid is divided into differential slices. The characteristic overflow length of each differential slice L_i is defined by the length of the gas–liquid interface and the characteristic velocity at the gas–liquid interface v_i is approximated by the velocity of the flask wall $v_i = 2\pi n d_i/2$. Eqs. (7)–(10) are thus applied to calculate the mass transfer coefficient of the bulk liquid $k^B_{L,i}$. The bulk contribution in Eq. (5) results by considering the specific mass transfer area a^B_i. The film contribution in Eq. (5) is calculated using Higbie's penetration theory. This approach will be termed as the "Gnielinski two sub-reactor model" in the following. Applying Gnielinski's boundary layer theory to model the mass transfer in the bulk liquid results in an average deviation of the model from the measured values of 14%, meaning a correlation factor of 1.14 for the very broad range of operating conditions investigated (not shown). The agreement between the model and measured values when applying the "Gnielinski two sub-reactor model" for the bulk liquid is slightly superior to the "Kawase and Moo-Young two sub-reactor model" for the bulk liquid.

The volumetric mass transfer coefficients $k_L a_{Model}$ of the "Kawase and Moo-Young two sub-reactor model" correspond well with those of the "Gnielinski two sub-reactor model" (data not shown). This is quiet remarkable considering that the modelling approach is absolutely different and both approaches require absolutely no fitting parameters. Only at low $k_L a$-values does the "Kawase and Moo-Young two sub-reactor model" show slightly higher values than the "Gnielinski two sub-reactor model". The "Gnielinski two sub-reactor model" accounts for mass transfer at laminar flow conditions, which the "Kawase and Moo-Young two sub-reactor model" does not account for. Even though the condition of isotropic turbulence for the "Kawase and Moo-Young two sub-reactor model" have been ensured [25,28], it can be questioned, whether this transition is actually well defined within the shake flask. Considering the fact that both models require no fitting parameters for the large number of operating conditions investigated the agreement with measurement values can be considered as being good. In the following results from the "Gnielinski two sub-reactor model" only will be further discussed.

The data points have up to now been considered irrespective of flask size, shaking diameter or flask volume. In the following the validity of the "Gnielinski two sub-reactor model" in dependency of the maximum flask diameter, shaking diameter and filling volume will be discussed to figure out in which conditions the new modelling approach still doesn't describe the true mechanisms correctly.

4.4.3. Influence of the flask volume

When regarding the parity plot differentiated by flask size, shown in Fig. 7, a clear tendency becomes visible: the smaller the flask volume, the greater the overestimation of the model values compared to the measuring values. Fig. 8a shows a representative comparison between the model and measurement $k_L a$-values in dependency of the shaking frequency and flask volume. It can be clearly seen that the agreement between the model and measurement values improves with increasing flask volume. In the 250 ml flask the agreement is very good, whereas in the 50 ml flask the agreement increases with shaking frequency.

Influence of the shaking diameter. No general tendency in dependency of the shaking diameter could be found between the model and measuring values (data not shown). The agreement between the model- and measurement values

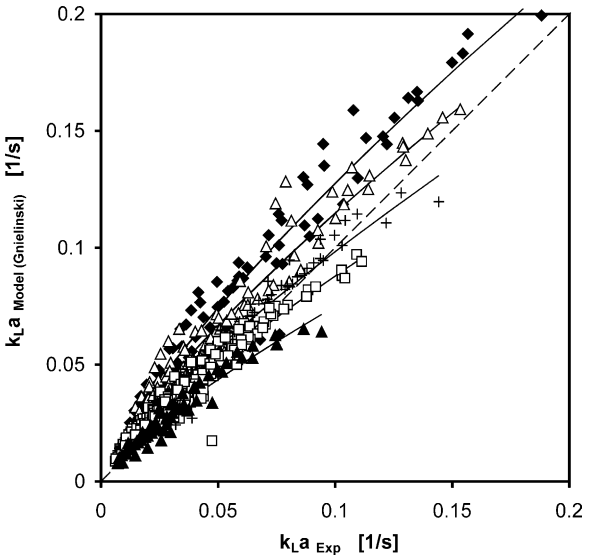

Fig. 7. Volumetric mass transfer coefficient of model $k_L a_{Model}$ (film mass transfer: Higbie, bulk mass transfer: Gnielinski) vs. measuring values $k_L a_{Exp}$ for different flask sizes: 50–1000 ml shake flask, 1.25–10 cm shaking diameter, 4–20% relative filling volume, 50–500 rpm shaking frequency, 1 M sodium sulphite system, $T = 22.5\,^{\circ}C$; flask sizes: (◆) 50 ml flask; (△) 100 ml flask; (+) 250 ml flask; (□) 500 ml flask; (▲) 1000 ml flask.

can be considered as being good for a shaking diameter of 5, 7 and 10 cm. The reason for small deviations between model- and measurement values at a shaking diameter of 2.5 cm (not shown), which decreases with increasing shaking frequency could not be found.

4.4.4. Influence of the filling volume

Fig. 8b shows a representative comparison between the model- and measurement $k_L a$-values in dependency of the shaking frequency and relative filling volume. It can be seen that the agreement between the model- and measurement values increases towards smaller relative filling volumes and increasing shaking frequencies.

There is a tendency in deviation between the "Gnielinski two sub-reactor model" and the measurement values in dependency of the maximum flask diameter, filling volume and shaking frequency. Still the agreement between the "Gnielinski two sub-reactor model" and the measurement values can be considered as being good, since no fitting parameters whatsoever are applied.

4.5. Gas–liquid mass transfer in liquid film

The rotating bulk liquid distributes a liquid film of a certain thickness δ on the flask wall and base. The dissolved oxygen concentration of the film at the time of application ($t_c = 0$) is equal to the dissolved oxygen concentration of the liquid bulk $c_{O_2,b}$. Gas–liquid mass transfer and reaction then takes place across the film for the contact time t_c, after which the liquid film is mixed under the rotating liquid bulk. This process is repeated continuously. As described earlier, Higbie's penetration theory is valid for semi-infinite space only, meaning that it describes the mass transfer as long as this takes place close to the gas–liquid interface. In the following the oxygen diffusion process into the liquid film will be considered time- and spatially-resolved to validate the application of Higbie's penetration theory in the "Gnielinski two sub-reactor model" as well as to investigate the influence of the reaction.

For a first estimation mass transfer for different contact times t_c equal to the reciprocal of the shaking frequency $1/n$ is considered. For example, t_c (100 rpm) $= 1/100 \times 60 = 0.6$ s. Contact times corresponding with shaking frequencies $n = 100$, 200, 300 and 400 rpm were considered. The reaction of the sodium sulphite system is considered as a 1.1 order reaction. In first investigations of the film thickness conducted using a fluorescent measuring method a film thickness in the order of $\delta = 5 \times 10^{-5}$ m was found in a 250 ml flask. In this preliminary measurement the film thickness was not investigated in dependency of the operating conditions. The oxygen mass balance in Eq. (11) was solved using the programme "gPROMS" applying the values listed in Table 1.The resulting profiles of the dissolved oxygen concentration $c_{O_2,L}(x,t)$ are shown in Fig. 9a. It can be seen that the lower the shaking frequency, meaning the higher the contact time t_c the higher the dissolved oxygen concentration at the flask wall. At high shaking frequencies ($n > 400$ rpm) the liquid film can still be considered as a semi-infinite space, meaning Higbie's penetration theory can still be applied. At low shaking frequencies the dissolved oxygen concentration at the flask wall is lifted, meaning that Higbie's penetration theory is no longer fully valid.

The relative deviation ε_{rel} between the oxygen flux calculated using Higbie's penetration theory (Eq. (14)) and that of the exact solution of Eq. (12) can be calculated according to:

$$\varepsilon_{rel} = \frac{\bar{\dot{n}}_{O_2} - \bar{\dot{n}}_{O_2,Higbie}}{\bar{\dot{n}}_{O_2}} \times 100 \qquad (21)$$

For the longest contact time considered $t_c = 0.15$ s (corresponding to $n = 400$ rpm) a relative deviation of $\varepsilon_{rel} = 2.6\%$ results. For the shortest contact time considered $t_c = 0.15$ s (corresponding to $n = 100$ rpm) a relative deviation of $\varepsilon_{rel} = 8.8\%$ results. This means that the higher the contact time, the more the actual oxygen flux (Eq. (12)) is actually underestimated by Higbie's theory (Eq. (14)). This is at first quite surprising, since based on the results presented in Fig. 9a Higbie would be expected to overestimate the actual oxygen flux. This indicates that there is a second influencing factor, which compensates the expected effect. This effect is that Higibe's penetration theory neglects the mass transfer due to the reaction in the liquid film.

To investigate the influence of the film thickness on the validity of Higbie's penetration theory, the film thickness was increased and decreased by 50% (meaning to $\delta = 7.5 \times 10^{-5}$

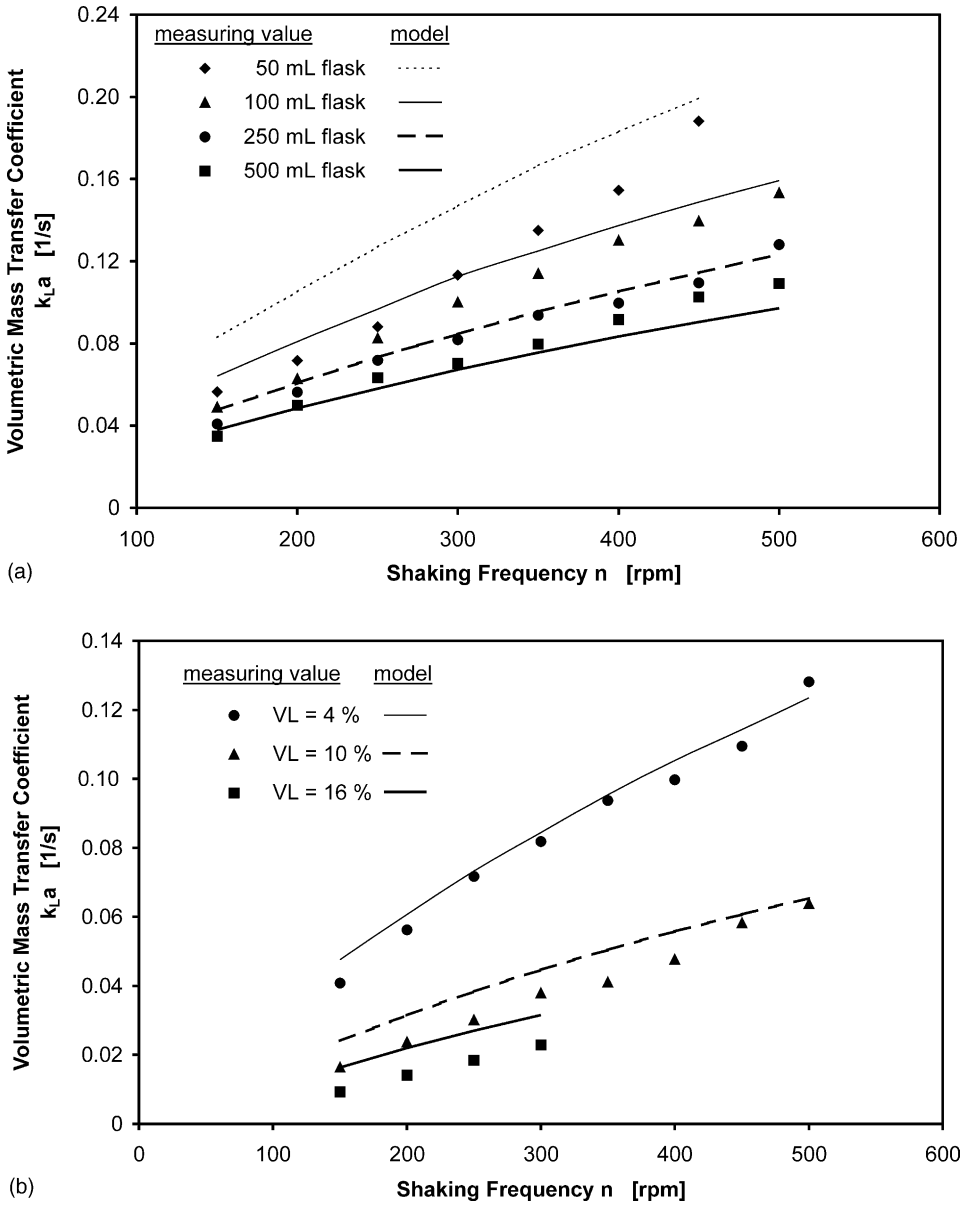

Fig. 8. Volumetric mass transfer coefficient of model $k_L a_{Model}$ (film mass transfer: Higbie, bulk mass transfer: Gnielinski) and measuring values $k_L a_{Exp}$ of 1 M sodium sulphite system, $T = 22.5\,^{\circ}C$ for: (a) different flask sizes, 5 cm shaking diameter, 4% relative filling volume; (b) different relative filling volumes in 250 ml flask, 5 cm shaking diameter.

and 2.5×10^{-5} m) and the resulting dissolved oxygen profile and oxygen flux calculated for a contact time of 0.6 s. From Fig. 9b it can be seen that the thinner the film, the more the dissolved oxygen concentration profile at the flask wall is lifted and the condition of semi-infinite space is certainly no longer given at $\delta = 2.5 \times 10^{-5}$ m. For $\delta = 2.5 \times 10^{-5}$ m a relative deviation of $\varepsilon_{rel} = -9.6\%$ results, meaning that Higbie's penetration theory actually overestimates the oxygen flux in thin films.

The above considerations have shown that the validity of Higbie's penetration theory depends sensitively on contact time and film thickness. Two general tendencies have been found

(i) at moderate contact times ($t_c > 0.2$ s) and film thickness ($\delta = 5 \times 10^{-5}$ m) the reaction within the film dominates and causes Higbie's penetration theory to underestimate the actual oxygen flux across the gas–liquid interface,
(ii) in thin liquid films ($\delta = 2.5 \times 10^{-5}$ m) the oxygen diffuses right through to the flask wall and the condition of semi-infinite space is no longer given; in this case Higbie's penetration theory overestimates the actual oxygen flux across the gas–liquid interface.

To elucidate the exact influence of the above tendencies on the deviations in the "Gnielinksi two sub-reactor model" shown above detailed measurements of the film thickness

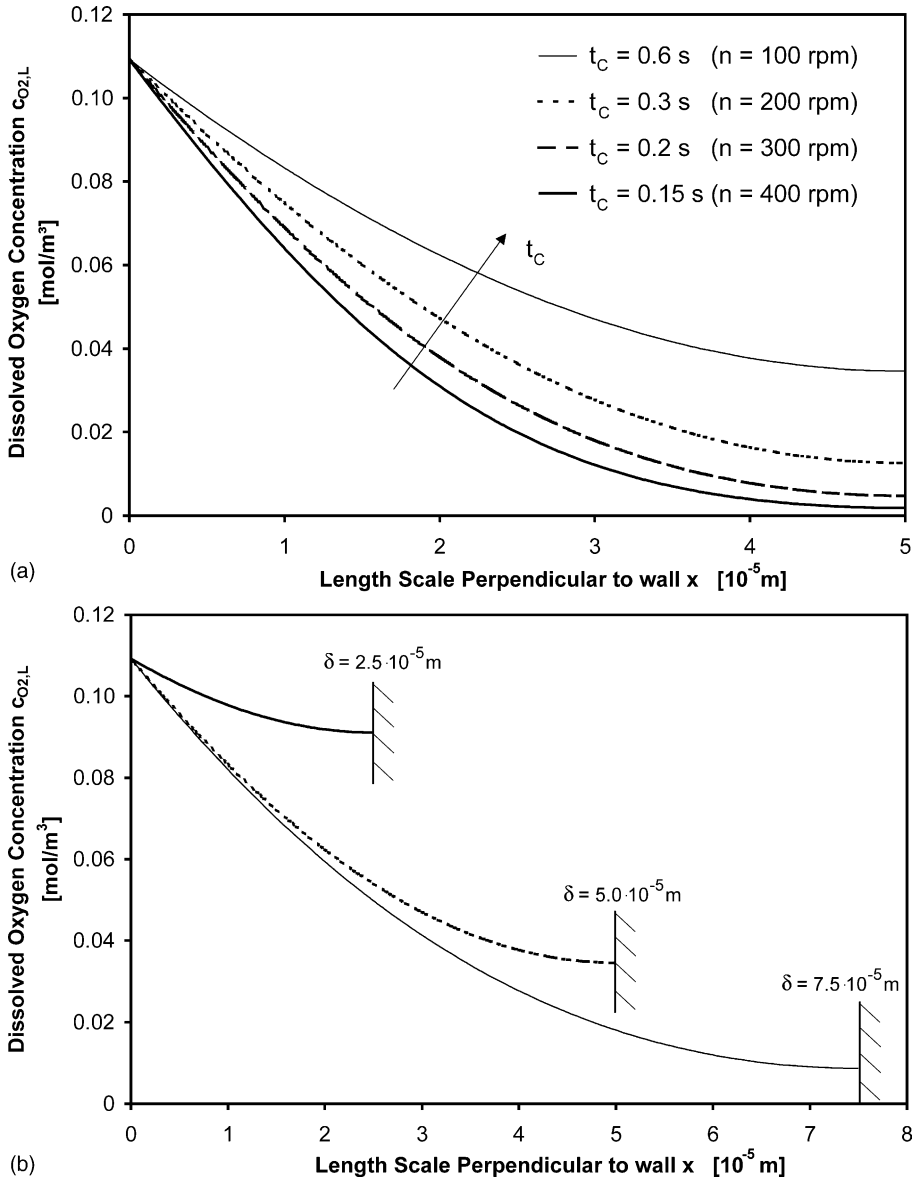

Fig. 9. Calculated oxygen concentration c_{O_2} in liquid film vs. penetration depth x. (a) Variation of the contact time t_c, film thickness $\delta = 5 \times 10^{-5}$ m. (b) Variation of the film thickness, contact time $t_c = 0.6$ s ($n = 100$ rpm).

are necessary, since the film thickness may be a function of the operating conditions such as shaking frequency and maximum flask diameter.

5. Conclusion

A fully mechanistic "two sub-reactor model" of the gas–liquid mass transfer in shake flasks at waterlike liquid viscosity has been developed. This model considers the shake flask as a "two sub-reactor" system dividing it into a hypothetical film reactor and a stirred tank reactor. The mass transfer into the liquid film (film reactor) on the flask wall is described using Higbie's penetration theory. The mass transfer into the bulk liquid (stirred tank reactor) is equally well described by two different mass transfer theories: that of Kawase and Moo-Young [26] and that of Gnielinski, which is based on the boundary layer theory [29] for a rigid boundary. Gnielinski's model can be considered to describe mass transfer at laminar flow conditions better than Kawase and Moo-Young's model. The models require no fitting parameters whatsoever and satisfactorily describe the measuring values of the volumetric mass transfer coefficient $k_L a$ and the maximum oxygen transfer capacity OTR_{max} in a 1 M aqueous sodium sulphite model system with an average deviation of 14%. The OTR_{max} of the sodium sulphite system has shown a constant correlation factor of 2.8 with an oxygen limited *P. pastoris* culture under variation of the operating conditions. Other biological systems have still to be investigated. Thus, the

developed model can be applied to chose suitable operating conditions for biological screening experiments at waterlike viscosities apriori to screening ensuring sufficient oxygen supply.

It could be shown that the validity of Higbie's penetration theory to describe the mass transfer in the liquid film sensitively depends on the film thickness and contact time between the gas and liquid phase. A more detailed investigation of the influence of the operating parameters on the film must be conducted.

The applicability of the model to higher liquid viscosities has to still be investigated. The liquid distribution in the flask becomes increasingly asymmetrical towards higher viscosities [23] and may finally reach an "out-of-phase" state. This effect is not accounted for by the presented model of the liquid distribution which is also the basis for calculating the mass transfer area. Furthermore, it can be assumed that the thickness of the liquid film on the flask wall increases with viscosity, resulting in a larger fraction of the liquid participating in film mass transfer. In our present model the film volume is neglected.

References

[1] M.D. Hilton, Small-scale liquid fermentations, in: A.L. Demain, J.E. Davies (Eds.), Manual of Industrial Microbiology and Biotechnology, American Society for Microbiology, Washington, 1999, pp. 49–60.

[2] J.C. Van Suijdam„ N.W.F. Kossen, A.C. Joha, Model for oxygen transfer in a shake flask, Biotechnol. Bioeng. 20 (1978) 1695–1709.

[3] T. Anderlei, J. Büchs, RAMOS (respiration activity monitoring system), Bioforum 3 (2001) 149–151.

[4] J. Büchs, Introduction to advantages and problems of shaken cultures, Biochem. Eng. J. 7 (2) (2001) 91–98.

[5] L.E. McDaniel, E.G. Bailey, A. Zimmerli, Effect of oxygen supply rates on growth of *Esherichia coli*. Part I. Studies in unbaffled and baffled shake flasks, Appl. Microbiol. 13 (1) (1965) 109–114.

[6] C. Mrotzek, T. Anderlei, H.-J. Henzler, J. Büchs, Mass transfer resistance of sterile plugs in shaking reactors, Biochem. Eng. J. 7 (2) (2001) 107–112.

[7] U. Maier, J. Büchs, Characterisation of the gas–liquid mass transfer in shaken bioreactors, Biochem. Eng. J. 7 (2) (2001) 99–106.

[8] Y. Hirose, H. Sonoda, K. Kinoshita, H. Okada, Studies on oxygen transfer in submerged fermentations. Part IV. Determination of oxygen transfer rate and respiration rate in shaken cultures using oxygen analysers, Agric. Biol. Chem. 30 (1) (1966) 49–58.

[9] H.-J. Henzler, M. Schedel, Suitability of the shake flask for oxygen supply to microbial cultures, Bioprocess Eng. 7 (1991) 123–131.

[10] V.B. Veljkovic, S. Nikolic, M.L. Lazic, C.R. Engler, Oxygen transfer in flasks shaken on orbital shakers, Hem. Ind. 49 (6) (1995) 265–272.

[11] C.T. Calam, Shake flask fermentations, in: A.L. Demain, N.A. Solomon (Eds.), Manual of Industrial Microbiology and Biotechnology, American Society for Microbiology, Washington, DC, 1996, pp. 59–65.

[12] F. Veglio, F. Beolchini, S. Ubaldini, Empirical models for oxygen mass transfer: a comparison between shake flask and lab-scale fermentor and application to manganiferous ore bleaching, Process Biochem. 33 (4) (1998) 367–376.

[13] R. Hermann, N. Walter, U. Maier, J. Büchs, Optical method for the determination of the oxygen transfer capacity of small bioreactors based on sulphite oxidation, Biotechnol. Bioeng. 74 (5) (2001) 355–363.

[14] J.E. Sawicki, C.H. Barron, On the kinetics of sulphite oxidation in heterogeneous systems, Chem. Eng. J. 5 (1973) 153–159.

[15] P.M. Wilkinson, B. Doldersum, P.H. Cramers, L.L. van Dierendonck, The kinetics of uncatalysed sodium sulphite oxidation, Chem. Eng. Sci. 48 (5) (1993) 933–941.

[16] V. Linek, V. Vacek, Chemical engineering use of catalyzed sulphite oxidation kinetics for the determination of mass transfer characteristics of gas–liquid contactors, Chem. Eng. Sci. 36 (11) (1981) 1747–1768.

[17] U. Maier, S. Lotter, J. Büchs, Calculation of the Liquid Distribution and Mass and Momentum Transfer Area in Shake Flasks on Rotary Shakers at Waterlike Viscosities, 2003, in press.

[18] R. Higbie, The rate of absorption of a pure gas into a still liquid during short periods of exposure, Trans. Am. Inst. Chem. Eng. 31 (1935) 365–389.

[19] K. Akita, Diffusivities of gases in aqueous electrolyte solutions, Ind. End. Chem. Fundam. 56 (20) (1981) 89–94.

[20] A. Schumpe, G. Quicker, W.D. Deckwer, Gas Solubilities in Microbial Culture Media, in Reaction Engineering, Springer, Berlin, 1982, pp. 1–37.

[21] T. Anderlei, J. Büchs, Device for sterile online measurement of the oxygen transfer rate in shake flasks, Biochem. Eng. J. 7 (2) (2001) 157–163.

[22] T. Anderlei, W. Zang, J. Büchs, Online respiration activity measurement (OTR, CTR, RQ) in shaking flasks, Biochem. Eng. J. (2003), this issue.

[23] J. Büchs, U. Maier, C. Milbradt, B. Zoels, Power consumption in shake flasks on rotary shaking machines. Part II. Non-dimensional description of specific power consumption and flow regimes in unbaffled flasks at elevated liquid viscosity, Biotechnol. Bioeng. 68 (6) (2000) 594–597.

[24] S. Lotter, J. Büchs, Utilization of specific power consumption measurements for optimization of culture conditions in shaking flasks, Biochem. Eng. J. (2003), this issue.

[25] J. Büchs, B. Zoels, Evaluation of the ratio of the maximum to specific power consumption in shaking bioreactors. Proceedings of the Third International Symposium on Mixing in Industrial Processes, J. Chem. Eng. Jpn. 34 (5) (2001) 647–653.

[26] Y. Kawase, M. Moo-Young, Mass transfer at a free surface in stirred tank bioreactors, Trans. IChemE 68 (Part A) (1990) 189–194.

[27] W.V. Pinczewski, S. Sideman, A model for mass (heat) transfer in turbulent tube flow. Moderate and high Schmidt numbers, Chem. Eng. Sci. 29 (PartA) (1974) 1969–1976.

[28] F. Liepe, W. Meusel, H.O. Möckel, B. Platzer, Weißgräber, Verfahrenstechnische Berechnungsmethoden, Teil 4 Stoffvereinigung in fluiden Phasen, VCH Publishers, Weinheim, 1988.

[29] V. Gnielinski, Berechnung mittlerer Wärme- und Stoffübergangskoeffizienten an laminar und turbulent überströmten Einzelkörpern mit Hilfe einer einheitlichen Gleichung, Forsch. Ing. Wes. 41 (5) (1975) 145–153.

[30] C.J. King, Turbulent liquid phase mass transfer at a free gas–liquid interface. Part I. And EC, Fundamentals 5 (1) (1966) 1–8.

[31] F. Kudrjawizki, M. Bauer, Gastransport durch die Oberfläche gerührter Flüssigkeiten, Chem. Ing. Technol. 65 (11) (1993) 1360–1362.

[32] C.L. Lamont, D.S. Scott, An eddy cell model of mass transfer into the surface of a turbulent liquid, AIChE J. 16 (1) (1970) 513–519.

[33] T.G. Theofanous, R.N. Houze, L.K. Brumfield, Turbulent mass transfer at free gas–liquid interfaces, with application to open-channel, bubble and jet flows, Int. J. Heat Mass Transfer 19 (1976) 613–624.

[34] B.D. Prasher, Gas absorption in a turbulent film, Chem. Eng. Sci. 28 (1973) 1230.

[35] Z. Zhang, C.R. Thomas, Eddy number distribution in isotropic turbulence and its application for estimating mass transfer coefficients, Chem. Eng. Commun. 140 (1) (1996) 207–217.